



1 The effect of myeloperoxidase isoforms on biophysical properties 2 of red blood cells

3 Ekaterina V. Shamova¹ · Irina V. Gorudko¹ · Daria V. Grigorieva¹ · Alexey V. Sokolov^{2,3,4} · Anatoli U. Kokhan¹ ·
4 Galina B. Melnikova⁵ · Nikolai A. Yafremau⁶ · Sergey A. Gusev⁴ · Anastasia N. Sveshnikova⁷ · Vadim B. Vasilyev^{2,3} ·
5 Sergey N. Cherenkevich¹ · Oleg M. Panasenko^{4,8}

6 Received: 22 March 2019 / Accepted: 8 November 2019
7 © Springer Science+Business Media, LLC, part of Springer Nature 2019

8 Abstract

9 Myeloperoxidase (MPO), an oxidant-producing enzyme, stored in azurophilic granules of neutrophils has been recently
10 shown to influence red blood cell (RBC) deformability leading to abnormalities in blood microcirculation. Native MPO is
11 a homodimer, consisting of two identical protomers (monomeric MPO) connected by a single disulfide bond but in inflam-
12 matory foci as a result of disulfide cleavage monomeric MPO (hemi-MPO) can also be produced. This study investigated if
13 two MPO isoforms have distinct effects on biophysical properties of RBCs. We have found that hemi-MPO, as well as the
14 dimeric form, bind to the glycoporphins A/B and band three protein on RBC's plasma membrane, that lead to reduced cell
15 resistance to osmotic and acidic hemolysis, reduction in cell elasticity, significant changes in cell volume, morphology, and
16 the conductance of RBC plasma membrane ion channels. Furthermore, we have shown for the first time that both dimeric
17 and hemi-MPO lead to phosphatidylserine (PS) exposure on the outer leaflet of RBC membrane. However, the effects of
18 hemi-MPO on the structural and functional properties of RBCs were lower compared to those of dimeric MPO. These find-
19 ings suggest that the ability of MPO protein to influence RBC's biophysical properties depends on its conformation (dimeric
20 or monomeric isoform). It is intriguing to speculate that hemi-MPO appearance in blood during inflammation can serve as
21 a regulatory mechanism addressed to reduce abnormalities on RBC response, induced by dimeric MPO.

22 **Keywords** Monomeric myeloperoxidase · Dimeric myeloperoxidase · Inflammation · RBC · Phosphatidylserine

A1 **Electronic supplementary material** The online version of this
A2 article (<https://doi.org/10.1007/s11010-019-03654-0>) contains
A3 supplementary material, which is available to authorized users.

A4 ✉ Ekaterina V. Shamova
A5 shamova@tut.by

A6 ¹ Belarusian State University, Minsk, Belarus

A7 ² FSBSI "Institute of Experimental Medicine", St. Petersburg,
A8 Russia

A9 ³ Saint-Petersburg State University, St. Petersburg, Russia

A10 ⁴ FSBI "Federal Research and Clinical Center of Physical-
A11 Chemical Medicine" FMBA, Moscow, Russia

A12 ⁵ A.V. Luikov Heat and Mass Transfer Institute of the National
A13 Academy of Sciences of Belarus, Minsk, Belarus

A14 ⁶ State Institution «N.N. Alexandrov Republican Scientific
A15 and Practical Center of Oncology and Medical Radiology»,
A16 Minsk, Belarus

A17 ⁷ Lomonosov Moscow State University, Moscow, Russia

A18 ⁸ Pirogov Russian National Research Medical University,
A19 Moscow, Russia

Introduction

Myeloperoxidase (MPO) is a cationic protein, which is most
abundantly expressed in azurophilic granules of neutrophils
(2–5% of the total cellular protein). It is a heme-containing
glycosylated oxidoreductase, which in addition to its per-
oxidase activity, catalyzes the production of (pseudo)hypo-
halous acids (halogenating activity), mainly hypochlorous
(HOCl), hypothiocyanous (HOSCN) and hypobromous
(HOBr) acids [1–4]. Being strong oxidants and halogenat-
ing agents, hypohalous acids interact with many biologi-
cally important molecules: nucleic acids, proteins, lipids,
carbohydrates, etc. [5, 6]. Due to this, MPO has a bacteri-
cidal function. However, excessive production of reactive
halogen-containing compounds (reactive halogen species)
can lead to host cell and tissue damage, initiating the devel-
opment of oxidative/halogenative stress and triggering a
number of diseases associated with inflammation [6–8].

MPO can also regulate the function of immune and non-immune cells via its nonenzymatic effects. MPO binding with the cell surface of platelets [9, 10], neutrophils [11, 12], and erythrocytes [13, 14] are able to activate the processes of intracellular signaling, leading to changes in the structural and functional properties of these cells.

Native MPO, released into the extracellular space as a result of neutrophil degranulation, is a homodimer, consisting of two identical protomers connected by a single disulfide bond, each containing light, heavy chains and heme [15]. Synthesis of dimeric MPO from monomeric ones is carried out at the stage of promyelocyte differentiation into granulocytes, as a result of which a dimeric glycosylated heme-containing MPO is formed [16, 17].

Under in vitro conditions, the monomeric form of MPO, termed hemi-myeloperoxidase (hemi-MPO), can be easily formed by a cleavage of disulfide bond by reduction and alkylation, linking two identical protomers in native MPO [18]. Recently, we have shown that monomeric MPO can be formed in vitro by HOCl-induced disulfide bond oxidation [19]. These results suggest the possibility of hemi-MPO formation in inflammatory foci, where the generation of reactive halogen species is increased and various redox reactions are initiated. Indeed, recently we have shown the presence of hemi-MPO in the plasma of patients with marked inflammation [20]. Under in vivo conditions, the appearance of hemi-MPO is also possible as a result of incomplete processing to the mature enzyme [16, 17].

One of current interest is the question of whether the functional properties of two MPO isoforms are different or similar and whether hemi-MPO, as well as the dimeric form, are able to bind to cell surface and regulate intracellular signaling processes.

Recently, we have shown that hemi-MPO induced cytosolic Ca^{2+} -rise, as well as lysozyme and elastase degranulation in human neutrophils, but these effects were much weaker than observed in the case of dimeric MPO [20]. It should be noted that hemi-MPO has the same as dimeric MPO peroxidase and chlorinating activity and retains its bactericidal ability [16, 17, 21].

In this work, we carried out a comparative analysis of the hemi-MPO (obtained by disulfide bond reduction in dimeric MPO) and dimeric MPO effects on the structural and functional properties of red blood cells (RBCs). We have shown that hemi-MPO, as well as the dimeric form, bind to the glycoporphins A/B and band 3 protein on RBC's plasma membrane, that led to changes in transmembrane potential, RBC morphology, reduced RBC deformability and reduced resistance to hemolysis. It was for the first time demonstrated that both dimeric and hemi-MPO induced the exposure of phosphatidylserine (PS) to the outer surface of the RBC membrane. However, all observed effects of hemi-MPO were significantly weaker than in the case of dimeric

MPO. According to these data, it is intriguing to speculate that decomposition of native MPO into monomers in vivo may serve as a regulatory mechanism aimed to correct RBC function under inflammatory conditions.

Materials and methods

Chemicals

4-Aminobenzoic acid hydrazide (4-ABH), sodium citrate, 4-chloro-1-naphthol, H_2O_2 , HEPES, ethylene glycol-bis(2-aminoethylether)-*N,N,N',N'*-tetraacetic acid (EGTA), phorbol 12-myristate 13-acetate (PMA), ionomycin were purchased from Sigma-Aldrich (St. Louis, USA). Sodium L-aspartate was from Alfa Aesar (Ward Hill, USA). High-affinity rat and rabbit polyclonal antibodies against human MPO were prepared as described previously [22]. HL-60, cell culture medium (RPMI-1640), and fetal calf serum (FCS) were purchased from BioloT Ltd (Saint-Petersburg, Russia).

Isolation of dimeric MPO

The HL-60 cell line (promyelocytic leukemia) was used as a source of dimeric MPO. MPO isolated from HL-60 was identical to MPO isolated from human neutrophils by size exclusion chromatography, SDS-PAGE, Western blotting, N-terminal sequence analysis and have the same peroxidase and chlorinating activities [23]. Cells were cultivated at 37 °C and 100% humidity in RPMI-1640 medium, containing 10% FCS, 2 mM glutamine and 25 mM HEPES buffer (pH 7.4), in roller bottles for suspension culture. Once a week, cells were sedimented by centrifugation at 1500 g, the pellet was resuspended in a minimum volume of fresh medium, and 1/5 of the volume of this cell suspension was transferred to a roller bottle containing fresh medium, while the remaining cells were washed three times with phosphate-buffered saline (PBS, 10 mM $\text{Na}_2\text{HPO}_4/\text{KH}_2\text{PO}_4$, 137 mM NaCl, 2.7 mM KCl, pH 7.4), resuspended in 2 volumes of 100 mM Na-acetate buffer (pH 4.7) and frozen. Dimeric MPO was isolated from the extract of thawed HL-60 cells lysed by ultrasound (44 kHz) and purified by affinity chromatography on heparin-Sepharose, hydrophobic chromatography on phenyl-Sepharose, and gel filtration on Sephacryl S-200 HR [24]. Using this method, it is possible to isolate a homogeneous preparation of dimeric MPO with a high specific activity and a purity index (A_{430}/A_{280}) greater than 0.85.

Preparation of hemi-MPO [25]

The hemi form of MPO was prepared by treating dimeric MPO (145 μM) with 2-mercaptoethanol (1:4 molar ratio of

MPO to 2-mercaptoethanol) for 30 min at 37 °C in 100 mM Na-carbonate buffer, pH 9.4, as described elsewhere [18, 25]. SH-groups were then blocked with iodoacetamide for 30 min at 4 °C (1:20 molar ratio of MPO to iodoacetamide). The resulting protein solution was concentrated in VivaSpin 20 ultrafiltration units (Sartorius, Germany) with a molecular weight cut-off of 30 kDa, with the buffer being exchanged for 100 mM Na-acetate buffer (pH 5.5). Traces of dimeric MPO were separated from hemi-MPO by gel filtration on a Sephacryl S-200 HR column (114 × 1.5 cm) equilibrated with 100 mM Na-acetate buffer (pH 5.5). SDS-PAGE in non-reducing conditions showed a complete absence of the dimeric form in hemi-MPO preparation. It was shown that there were no differences in peroxidase, chlorinating and bactericidal activity between hemi-MPO and dimeric MPO [25]. Concentration of dimeric and hemi-MPO was determined spectrophotometrically using an extinction coefficient of 112,000 M⁻¹·cm⁻¹ per heme of MPO.

Isolation of RBCs

Washed RBCs were obtained after two centrifugation cycles at 400 g for 5 min of capillary blood (100 µl) in 10 ml of PBS or venous blood collected in tubes containing 3.8% (w/v) sodium citrate as anticoagulant at a ratio of 9:1 and stored in PBS, containing 10 mM D-glucose at 4 °C. Washed RBCs from capillary blood (1% hematocrit, unless otherwise indicated) were used for AFM, hemolysis, patch-clamp and flow cytometry assays whereas washed RBC from venous blood were used to prepare RBC ghosts (RBCGs) by hypoosmotic hemolysis. Venous blood samples were obtained from healthy donors at Federal State Budgetary Scientific Institution "Institute of Experimental Medicine". All blood donors were volunteers and gave informed consent.

RBCGs preparation

Washed RBCs were mixed with cold hemolysis buffer (10 mM Tris-HCl, 1 mM EDTA, pH 7.6, 4 °C) at a 1:20 ratio by volume and incubated at 4 °C for 5 min. Then, the sample was centrifuged twice at 30,000×g (30 min, 4 °C) and the RBCG pellet was resuspended with cold hemolysis buffer: by 10 volumes (first centrifugation) and by 3 volumes (second centrifugation). The final RBCG suspension was used for downstream procedures.

Detection of MPO-binding proteins using ligand western blot assay

RBCGs were lysed in SDS-Tris sample buffer (125 mM Tris-HCl, pH 6.8, 2% SDS, 0.1% 2-mercaptoethanol, 0.001% bromphenol blue, and 50% glycerol) at a ratio 1:5 by volume, and 100 µg of total protein was loaded per well of

polyacrylamide gel [26]. Using a semi-dry method [27] the separated proteins were transferred on nitrocellulose membranes and the blocking procedure was performed using a blocking solution BSA-T (1% BSA and 0.05% Tween 20 in PBS). To detect RBC proteins, which bind with MPO isoforms, the membranes were incubated for 30 min with hemi- or dimeric MPO in BSA-T solution, followed by exposure for 1 h to HRP-labeled rabbit anti-human MPO antibody. Each step was accompanied by washing of the membranes three times with BSA-T solution for at least 5 min per washing step. The peroxidase activity was visualized using 4-chloro-1-naphthol plus H₂O₂ system. In the absence of HRP-labeled antibody, basal MPO peroxidase activity was not manifested. There were no difference between MPO and hemi-MPO in binding to the HRP-labeled antibody against MPO as was shown in control dot-blotting experiments. The identity of MPO-binding protein bands on SDS-PAGE gels was confirmed by mass spectrometry after in situ tryptic digestion [28].

Hemolysis detection

A suspension of washed RBCs (30 µl) treated or not with monomeric/dimeric MPO was added to 60 mM NaCl solution (300 µl) to induce hypotonic hemolysis or to phosphate-citrate buffer containing 155 mM NaCl and 4.1 mM Na₂HPO₄/7.9 mM citric acid (300 µl) to induce acidic hemolysis. The process of hemolysis was recorded as changes in light transmission at 670 nm and 37 °C of constantly stirred cell suspensions using analyzer AP2110 (SOLAR, Minsk, Belarus). To quantify the hemolysis process the following parameters were used: *G*, maximal extent of hemolysis, i.e., the maximal level of light transmission of cell suspension at the plateau, and *t*₅₀, the time point when the change in light transmission has reached its half-maximal value.

Atomic force microscopy (AFM) measurements

RBCs were treated with monomeric/dimeric MPO for 10 min at room temperature and then fixed in 1.5% glutaraldehyde for 30 min. Fixed RBCs were washed by four-step centrifugation at 400 g for 3 min and the RBC pellet was resuspended twice in PBS and twice in distilled water. Washed RBCs were placed on a glass slide and air-dried for several hours. All steps were performed at room temperature.

The images of RBC's surface membrane were obtained using a NT-206 microscope (MicroTestMachines, Minsk, Belarus) working in the contact mode using the software of the microscope. Standart cantilevers NSC 11A («Mikro-Masch» Co, Estonia) with a spring constant of 3 N/m were used. Tip radii were checked by using a standard TGT01 silicon grating from NT-MDT (Moscow, Russia) and were

234 10 nm for topography visualization and 60 nm for cell stiff-
 235 ness determination. Surface profiles were obtained using
 236 scan sizes of 14×14 mm at a scan rate of 3 Hz. The result-
 237 ing image (topographic image) was recorded as a surface
 238 height distribution $Z(X, Y)$. For each scanned cell, the height
 239 H (maximum cell height), the concave depth h (minimum
 240 height of the cell), the diameter of RBC – d and the relative
 241 concave depth – k were determined: $k = (H-h)/h \cdot 100\%$.

242 The force spectroscopy regime was used to determine
 243 local elastic properties of RBCs. At least three force curves
 244 from the peripheral part of the randomly selected cells (7–10
 245 cells) for each treatment were recorded. The cell Young's
 246 modulus was calculated as described earlier [29] using Hertz
 247 model and used as a measure of RBC stiffness. The indenta-
 248 tion depth was 15 nm to avoid the influence of a rigid sub-
 249 strate on the magnitude of the estimating Young's modulus
 250 [30].

251 Light microscopy

252 To observe changes in RBC morphology, induced by MPO
 253 isoforms, RBCs were suspended in PBS, pH 7.4, with 1 mM
 254 CaCl_2 , placed in a Petri dish and transferred to an optical
 255 microscope for analysis. The transmitted light images of
 256 the RBCs were recorded before (control) and after MPO
 257 addition to cell suspension at time intervals of 15–60 s for
 258 15 min using an optical microscope Olympus BX51WI
 259 (Tokyo, Japan), LUMPlan objective ($40 \times / 0.80$) and digi-
 260 tal camera OSCAR 45 (Taiwan). Quantitative analysis was
 261 performed using the analyzer Mecos-Hemo (Mecos, Russia)
 262 counting approximately 500 cells per each image.

263 Measurement of RBC membrane potential 264 by patch-clamp technique

265 Washed RBCs (5 μl) were carefully placed in the bottom
 266 of a Petri dish, filled with 5 ml of external buffer solu-
 267 tion (145 mM NaCl, 10 mM HEPES, 10 mM D-glucose,
 268 5 mM KCl, 1 mM MgCl_2 , 1 mM CaCl_2 , pH 7.4, osmolarity
 269 290 mOsm). Patch pipettes with tip resistance 10–20 M Ω
 270 were prepared from borosilicate glass before each experi-
 271 ment using a puller Sutter P-97 (HEKA Elektronik, GmbH)
 272 and filled with internal buffer solution (5 mM NaCl, 10 mM
 273 HEPES, 145 mM KCl, 1 mM MgCl_2 , 0.3 mM CaCl_2 , 3 mM
 274 EGTA, pH 7.2, osmolarity 280 mOsm). A micromanipula-
 275 tor MP-225 (Sutter Instrument) was used to bring the patch
 276 pipette close to a single RBC and then a small negative
 277 pressure was applied to the pipette, leading to giga-seal for-
 278 mation (3–10 G Ω). Patch-clamp recordings of membrane
 279 potential were carried out in cell-attach configuration in cur-
 280 rent-clamp mode using an amplifier HEKA EPC 8 (HEKA
 281 Elektronik, GmbH), filtered at 1 kHz. When the success-
 282 ful cell-attached configuration was achieved and membrane

potential reached the constant values (15–20 mV), dimeric
 or hemi-MPO was added to bath solution and changes in
 membrane potential were recorded.

Flow cytometry

To probe PS exposure, washed RBCs were suspended at
 0.015% hematocrit in PBS, pH 7.4, with 2 mM CaCl_2 ,
 treated with monomeric/dimeric MPO or ionomycin/PMA
 for 15 min at room temperature, stained with Annexin
 V-Alexa Fluor 647 (100 $\mu\text{g}/\text{ml}$) under protection of light for
 5 min at room temperature and used immediately for flow
 cytometry assay. PS exposure was measured in the FL-6
 channel (660 nm) excited at 638 nm. 10,000 cells were
 measured per each sample.

To measure intracellular Ca^{2+} , RBCs were incubated with
 3.5 μM Fluor-3/AM in PBS for 60 min at 37 °C in the dark,
 followed by centrifugation (300 g, 7 min) and subsequent
 washing in PBS three times. Fluor-3-loaded RBCs were
 exposed to 100 nM of hemi-MPO or 100 nM of dimeric
 MPO or 1 μM of ionomycin (as a positive control) and the
 aliquots were sampled every minute to detect changes in
 Fluor-3 fluorescence (525 nm) excited at 488 nm.

Both flow cytometric assays were performed on a Navios
 (Beckman Coulter, USA) system.

Statistical analysis

Data are expressed as mean \pm SD or mean \pm SEM, as indi-
 cated in the captions to the figures and tables. To analyze dif-
 ferences between mean values of the two groups, the Student
 t test was used. Differences between mean values of more
 than two groups were analyzed by ANOVA followed by Stu-
 dent–Newman–Keuls test. Statistical analysis was performed
 using Origin 7.0 (Northampton, USA) or Statistica software.
 A p value < 0.05 was considered to be significant.

Results

Interaction of RBCG proteins with hemi-MPO

Recently, it was shown that binding of dimeric MPO to RBC
 surface is based mostly on electrostatic interactions with the
 participation of sialic acids and its main targets are band 3
 protein (B3) and glycophorin A and B [13, 31]. To check
 if hemi-MPO binds to the same targets on RBC surface,
 RBCG proteins were separated by SDS-PAGE (Fig. 1, panel
 1) and transferred to a nitrocellulose membrane. Their inter-
 action with hemi-MPO and dimeric MPO were analyzed
 using ligand Western blotting, using rabbit anti-MPO anti-
 bodies labeled with horseradish peroxidase. Rabbit antibod-
 ies against MPO did not react with RBCG proteins without

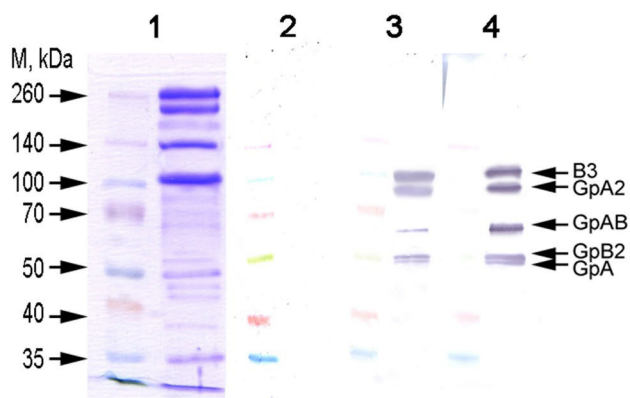


Fig. 1 Binding of human MPO to RBCG proteins. Prestained protein marker (the left lanes in each panel) and RBCG proteins (100 μ g per line) separated by SDS-PAGE and transferred on nitrocellulose membranes: panel 1—Coomassie brilliant blue R-250 staining; panel 2, 3 and 4—ligand Western blot staining using: no MPO (panel 2), 200 nM dimeric MPO (panel 3) and 200 nM hemi-MPO (panel 4) and horseradish peroxidase (HRP)-labeled rabbit anti-human MPO antibody (10 μ g/ml) of membranes. Arrows represent protein standards (on the left) or positions of specific RBCG proteins and their dimers (on the right)

preliminary addition of MPO (Fig. 1, panel 2). The membrane showed that five dimeric MPO-binding regions were revealed using ligand Western blot assay (Fig. 1, panel 3) corresponding to the band 3 protein (B3) and glycoprotein A and B (GpA2, GpAB, GpB2, GpA). These glycoproteins were identified earlier with help of periodic acid-Schiff reagent and by mass-spectrometry [13]. Similar patterns of hemi-MPO binding to the five protein areas were detected (Fig. 1, panel 4). These results indicate that hemi-MPO as well as the dimeric MPO binds to the band 3 protein and glycoprotein A and B of the RBC plasma membrane.

To be sure that hemi- and dimeric MPO stably bind to RBC surface proteins in their native environment, we incubated washed RBCs with MPO isoforms for 15 min and then measured MPO concentration in cell supernatants as described earlier [32]. The decrease of dimeric MPO as well as hemi-MPO content in cell supernatant (Supplementary Materials, Fig.S1) indicates that both isoforms stably bind with RBCs.

Effect of hemi-MPO on the RBC elastic properties and their resistance to hemolysis

Hemolysis was initiated by reducing the ionic strength of the medium (osmotic hemolysis) or pH (acidic hemolysis). As shown in Fig. 2a, b hemi-MPO as well as dimeric MPO augmented acidic and osmotic hemolysis in a dose-dependent manner. Thus, the degree of osmotic hemolysis (Fig. 2c) increased, and the half-time of acidic hemolysis decreased (Fig. 2d) for RBCs treated with both MPO forms

in comparison to control, indicating a decrease in cell resistance to hemolysis. However, the effect of hemi-MPO was lower in comparison with native dimeric MPO (Fig. 2c, d). It should be noted, that unrelated to MPO positively charged protein human lactoferrin (hLF) with molecular mass 76 kDa similar to that of hemi-MPO did not affect acidic and osmotic hemolysis (data not shown) indicating the specificity of MPO isoforms' effect on RBC resistant to hemolysis.

As MPO can induce the production of hypohalous acids, which are known to initiate RBC hemolysis [33, 34], we next examined the observed effects in the presence of MPO enzymatic activity inhibitor – 4-ABH. As shown in Fig. 2e 4-ABH (50 μ M) failed to abrogate hemi-MPO-mediated increase in hemolysis. Furthermore, under hypotonic and acidic conditions (used in present study) MPO peroxidase activity decreased by at least 97%. ABH (50 μ M) almost completely suppressed the rest of MPO enzymatic activity (data not shown).

Differences in the hemi-MPO and dimeric MPO effects on RBC mechanical properties were also shown by AFM. To assess the RBC surface elastic properties and cell stiffness, we determined the local Young's modulus for intact RBCs and RBCs treated with both MPO isoforms (Fig. 2f). Hemi-MPO and dimeric MPO caused increase of Young's modulus values by approximately 10% and 30%, respectively (Fig. 2f). These data indicate that both MPO isoforms lead to RBC membrane stabilization and increase in their mechanical stiffness but to a various stage.

Thus, it can be concluded, that binding of hemi-MPO, as well as native MPO with RBC plasma membrane, initiates similar changes in cell structural and functional properties. These hemi-MPO effects do not depend on the catalytic activity of the enzyme and are rather weaker than in the case of dimeric MPO.

Effect of hemi-MPO on size and morphology of RBCs

We have recently shown that RBC treatment with native dimeric MPO led to their volume increase, as evidenced by a marked increase in the number of stomatocytes and microspherocytes [13]. Moreover, the maximum change in cell morphology occurred within the first two min and then the cells reverted back to the morphology of normocytes. In this work, we examined the effect of hemi-MPO on cell morphology and compared it with the effect of dimeric MPO.

During the period of observation (15 min) the morphology of control (untreated) RBCs did not change over time. As expected dimeric MPO addition to RBCs suspension induced cell swelling during the first 15 s as was evidenced by appearance of significant amounts of stomatocytes (Fig. 3e), reduction in echinocyte number (Fig. 3b) and after 15 min of observation led to significant rise in the number

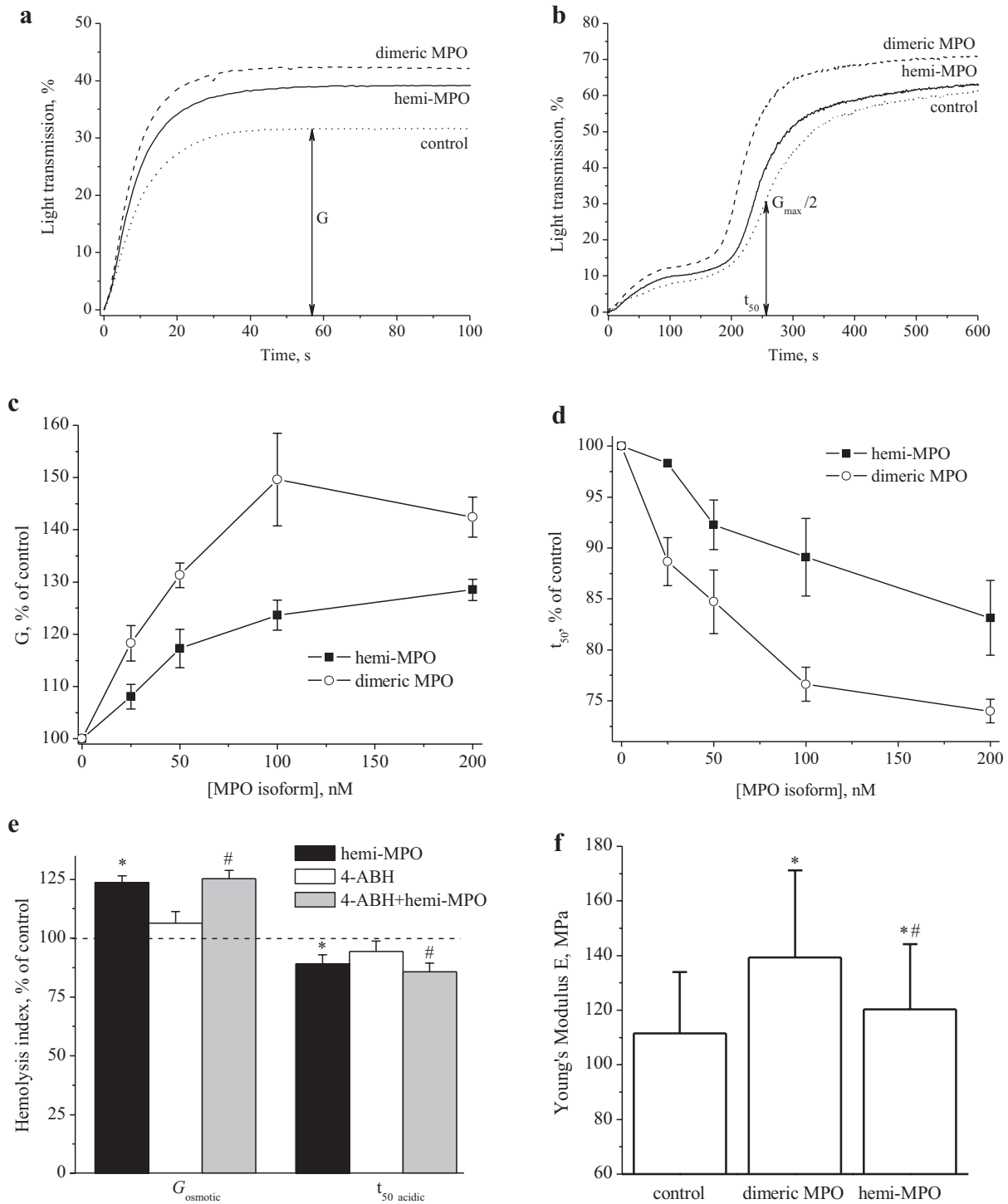


Fig. 2 Effects of MPO isoforms on hemolysis and RBC membrane elasticity. **a**, **b** Typical kinetics of osmotic (60 mM NaCl) (**a**) and acidic (4.1 mM Na₂HPO₄/7.9 mM citric acid, 155 mM NaCl; pH 2.9) (**b**) RBC hemolysis in the absence (control) and presence of dimeric and hemi-MPO (100 nM). **c**, **d** The degree (G) and the half-time (t_{50}) of osmotic (**c**) and acidic (**d**) hemolysis in the presence of different concentration dimeric and hemi-MPO. **e** The effect of specific inhibitor of MPO enzymatic activity 4-ABH (50 μ M) on the degree of

osmotic (G_{osmotic}) and the half-time of acidic ($t_{50 \text{ acidic}}$) RBC hemolysis in the presence of hemi-MPO (100 nM). The hemolysis index of control MPO untreated RBCs was 100%. **f** The influence of MPO isoforms (25 nM) on the Young's modulus of RBCs. The data are presented as mean \pm SD [$n=3-5$ (**a-e**) or $n=23-26$ (**f**)]. * $p < 0.05$ compared to control, # $p < 0.05$ compared to the effect of 4-ABH (**e**) or dimeric MPO (**f**)

Fig. 3 Changes in RBC morphology after incubating the cells with dimeric MPO (100 nM) or hemi-MPO (100 nM). The number (in %) of normocytes (a), echinocytes (b), cup-shaped cells (c), microspherocytes (d) and stomatocytes (e) was calculated for 15 s, 2 min, and 15 min after MPO addition. The data are presented as mean \pm SEM ($n=500-550$). * $p < 0.05$ comparing means to untreated control

of microspherocytes (Fig. 3d). Although hemi-MPO did not induce significant changes in the number of stomatocytes and echinocytes (Fig. 3e, b), the final increase in the number of microspherocytes was significant (Fig. 3d), however, this effect was less pronounced than in the case of dimeric MPO.

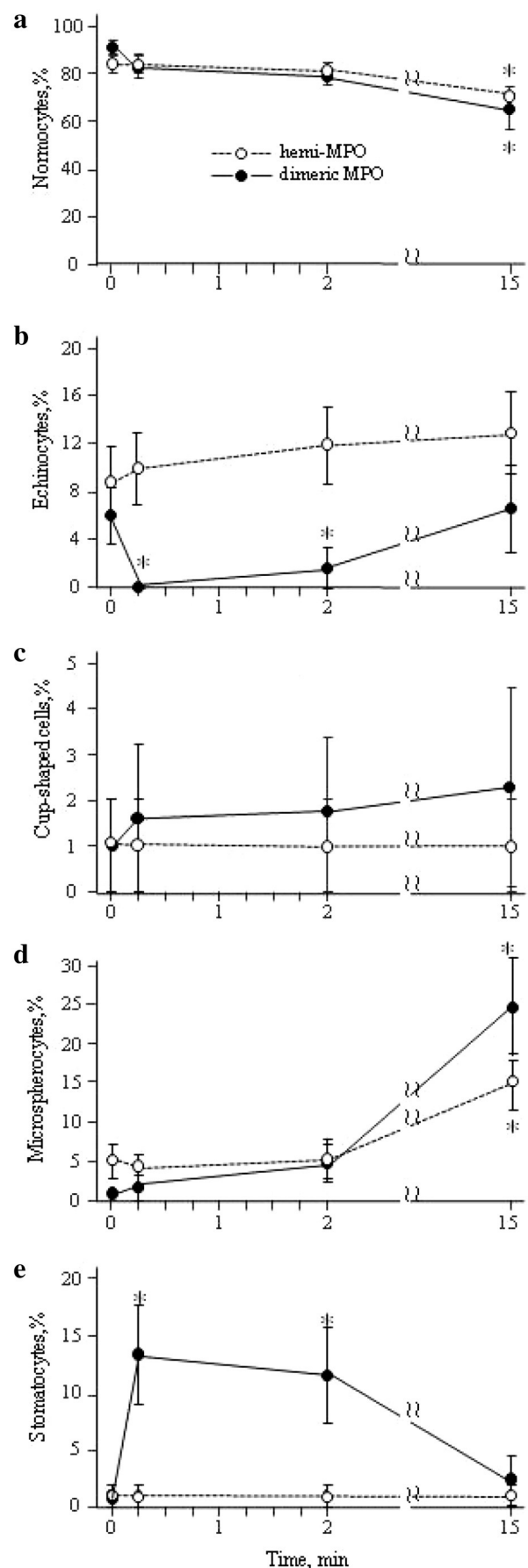
It should be noted that the observed appearance of microspherocytes in cell suspension indicates about the MPO-induced increase in cell volume. Indeed, changes in RBC volume, induced by both MPO isoforms, were observed by AFM (Fig. 4, Table 1). It was shown that RBCs treatment with dimeric MPO led to a decrease in concave depth, as evidenced by a significant change in the parameters h and k , while other linear cell sizes (height, H and diameter, d) were unaffected (Table 1, Fig. 4c). In the presence of hemi-MPO, a decrease of the relative concave depth (k) was also observed, however, this change was lower, compared to native dimeric MPO (Fig. 4).

Thus, the obtained results indicate that hemi-MPO, similarly to the dimeric isoform of the enzyme, induces changes in RBC morphology and increase in their volume, but to a much lesser extent than dimeric MPO.

428 Hemi-MPO effect on RBC membrane potential

Changes in morphology and RBC volume are closely linked to ionic conductivity of plasma membrane. Thus, recently, we have shown that MPO-induced increase in RBC volume is associated with depolarization of plasma membrane, while the subsequent restoration of cell morphology and volume—with plasma membrane hyperpolarization [13]. In the present work, we also examined whether hemi-MPO had an influence on RBC membrane potential. Using a “cell-attach” patch clamp technique, it was shown, that like in the case with dimeric MPO, the addition of hemi-MPO to RBC suspension induced a two-stage change in membrane potential: fast membrane depolarization, followed by a prolonged hyperpolarization (more than 10 min) (Fig. 5a). As expected, the effect of hemi-MPO at both stages: depolarization and hyperpolarization were lower compared to dimeric isoform of MPO (Fig. 5a, b).

It should be noted, that all described changes in structural and functional properties of RBCs, induced by both MPO isoforms, were observed only in the medium containing Ca^{2+} ions. No apparent changes in morphology, cell sizes or ion permeability occurred in calcium-free medium (data not shown). Actually, we have shown previously [13], that



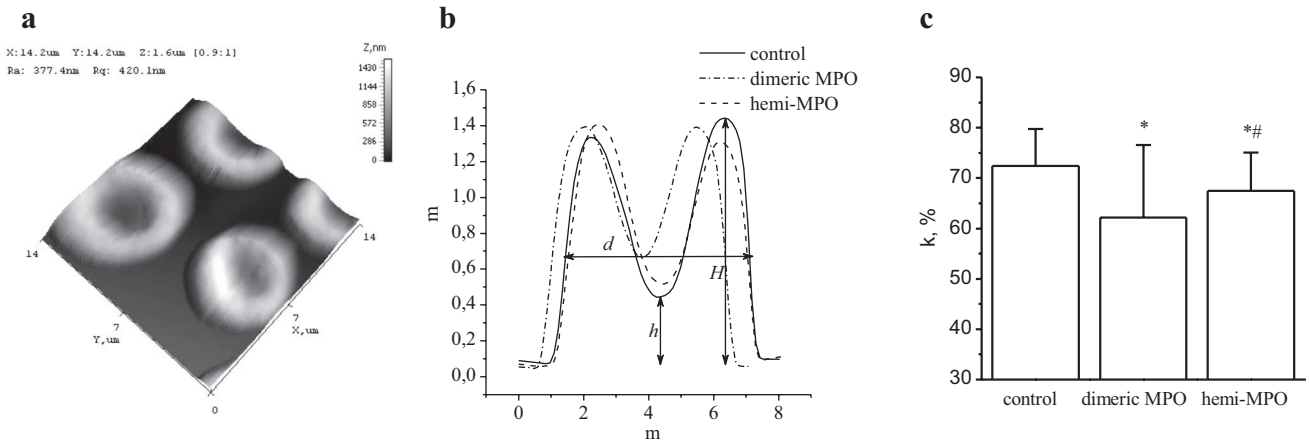


Fig. 4 AFM-images and surface topography of RBCs. **a** AFM 3D-image of RBCs fixed with 1.5% glutaraldehyde for 30 min. **b** The profiles of the RBC treated with dimeric MPO (100 nM), hemi-MPO (100 nM), or the vehicle (control), used to calculate cell diameter – d maximal cell height (H), concave height (h), and relative concave

depth, calculated as: $k = (H-h)/h \cdot 100\%$. **c** Changes in the relative concave depth of the RBC (k) after 2 min incubation with dimeric or hemi-MPO (100 nM). The data are presented as mean \pm SD ($n = 52-58$). * $p < 0.05$ comparing means to untreated control, # $p < 0.05$ comparing means to the effect of dimeric MPO

Table 1 Changes in RBC size in the presence of dimeric and hemi-MPO (100 nM)

	$H, \mu\text{m}$	$h, \mu\text{m}$	$d, \mu\text{m}$
Control	1.36 ± 0.15	0.40 ± 0.15	5.64 ± 0.29
Dimeric MPO	1.36 ± 0.14	$0.51 \pm 0.43^*$	5.45 ± 0.36
Hemi-MPO	1.35 ± 0.15	$0.42 \pm 0.08^\#$	5.46 ± 0.46

H RBC height (maximum height of the cell), h RBC concave height (minimum height of the cell), d RBC diameter. The data are presented as mean \pm SD ($n = 52-58$) * $p < 0.05$ compared with control, # $p < 0.05$ compared with the effect of dimeric MPO

binding of native MPO to RBC plasma membrane induces Ca^{2+} entry into the cytosol of cells. In present work, hemi-MPO was also capable to induce rise in cytosolic Ca^{2+} concentration as measured by flow cytometry in Fluor-3 loaded RBCs (Fig. 6) but this effect was lower compared to the Ca^{2+} -response induced by dimeric MPO and Ca^{2+} -ionophore ionomycin.

Since intracellular Ca^{2+} -rise can activate phospholipid scramblase, that bidirectionally and nonspecifically transports phospholipids, leading to PS exposure on cell external

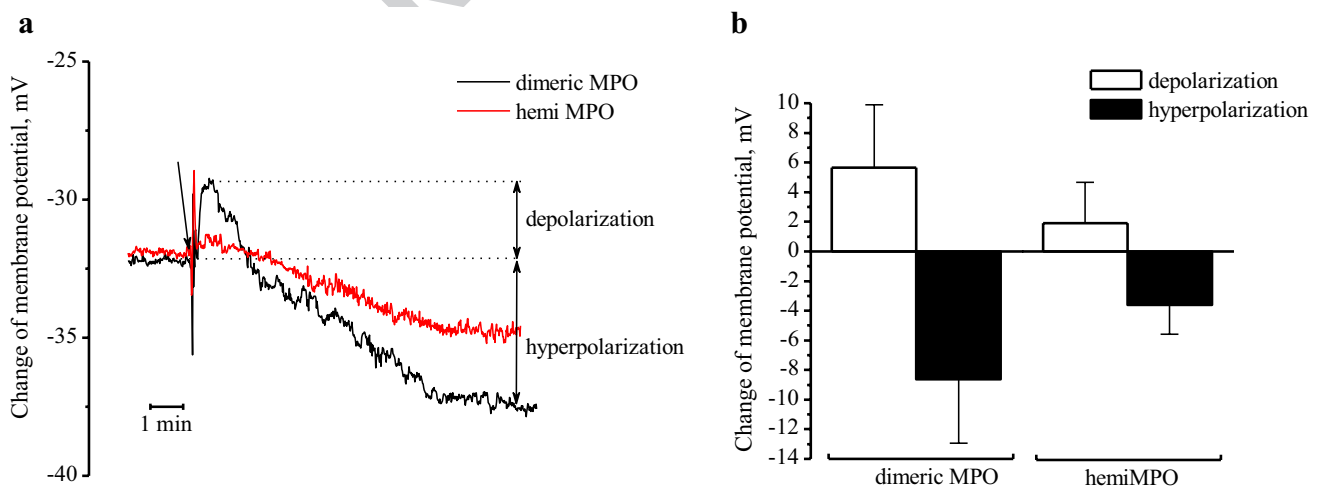


Fig. 5 Effect of MPO isoforms on RBC membrane potential. **a** The kinetics of membrane potential induced by dimeric or hemi-MPO (100 nM), which show depolarization and hyperpolarization phases. **b** Values of depolarization and hyperpolarization effects of MPO

isoforms on RBC membrane potential. Arrow indicates the moment of MPO isoform addition. The data are presented as mean \pm SD ($n = 7-8$)

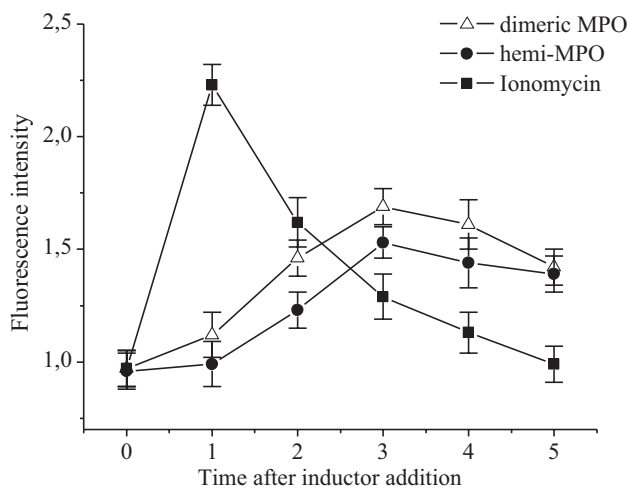


Fig. 6 Effect of MPO isoforms on cytosolic Ca^{2+} concentration. Changes in mean fluorescence intensity of Fluor-3 loaded RBCs, treated with dimeric MPO (100 nM), hemi-MPO (100 nM) or ionomycin (1 μM), detected by flow cytometry assay. The data are presented as mean \pm SD ($n=3-5$)

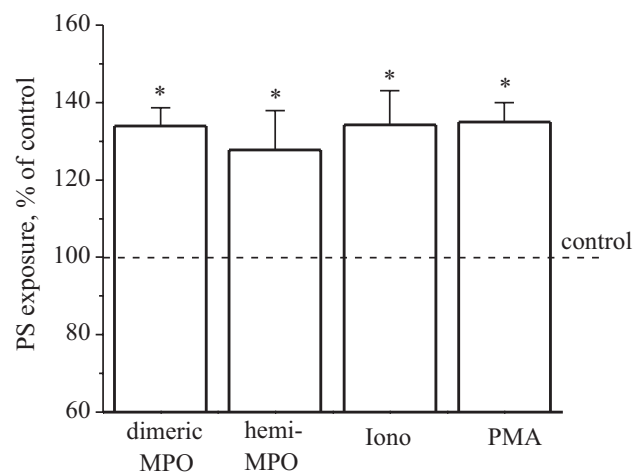


Fig. 7 Effect of MPO isoforms on PS exposure on the outer leaflet of RBCs. Prior annexin V-Alexa Fluor 647 staining RBCs were pre-treated with dimeric MPO (100 nM), hemi-MPO (100 nM), PMA (5 μM), ionomycin (1 μM) or the vehicle (control) for 15 min at room temperature in PBS, containing 2 mM CaCl_2 . PS exposure (Annexin V binding) was determined by change in mean fluorescence intensity, % of control. The data are presented as mean \pm SD ($n=3-4$). * $p < 0.05$ comparing means to untreated control

461 leaflet [35] and considering recent data, that PS expo-
 462 sure is controlled by membrane hyperpolarization due to
 463 Ca^{2+} -dependent Gardos channel opening [36], it was intriguing
 464 to investigate if native dimeric and hemi-MPO lead to
 465 PS exposure on the RBC's membrane.

466 PS exposure in RBCs, treated with dimeric 467 and hemi-MPO

468 To determine if MPO isoforms are able to induce PS expo-
 469 sure on the outer RBC's leaflet, cells were preincubated with
 470 native dimeric or hemi-MPO for 15 min and stained with
 471 annexin V for PS detection by flow cytometry. As a positive
 472 control, we used calcium ionophore ionomycin (1 μM) and
 473 PKC activator PMA (5 μM), which were shown to induce
 474 PS exposure in RBCs [36–38]. As shown on Fig. 7 RBC
 475 treatment with both dimeric MPO and hemi-MPO led to a
 476 significant increase in PS exposure by 34% and 22%, respec-
 477 tively. The effect of dimeric MPO was comparable to that
 478 of ionomycin and PMA. However, according to the previous
 479 results, the effect of hemi-MPO was less pronounced.

480 Discussion

481 Today, along with wide investigation of MPO enzymatic
 482 activity, great attention is paid to its ability to bind to plasma
 483 membrane of blood cells and regulate their structural and
 484 functional properties. This ability doesn't depend on the
 485 catalytic activity of the enzyme, but is largely due to the
 486 peculiarities of the structure of the MPO molecule. In this

work, we have shown, that the decomposition of dimeric
 MPO into monomers is accompanied by a decrease in its
 ability to regulate the structural and functional properties
 of red blood cells.

The peculiarity of MPO structure is that mature MPO,
 which is stored in azurophilic granules of fully differentiated
 neutrophils, is a dimer (~145 kDa), consisting of identical
 heme-containing protomers connected by a disulfide bond.
 Native dimeric MPO is able to bind to the plasma membrane
 and regulate the functional responses of various cells.

Thus, binding of native MPO to CD11b/CD18, a major
 neutrophil adhesion receptor, leads to tyrosine phospho-
 rylation of a number of proteins and as a result stimulates
 degranulation [12], adhesion, and also increases the survival
 of these cells [39]. However, as has been shown previously
 [20], abnormal MPO conformation is accompanied by a
 decrease in its ability to regulate the functional activity of
 neutrophils. The reductive alkylation of MPO leads to its
 inability to enhance neutrophil adhesion [40]. Recently, we
 have shown that hemi-MPO, as well as MPO modified by
 hypochlorous acid (MPO-HOCl), lost its ability to prime
 NADPH-oxidase of neutrophils [20]. In addition, it was
 found that hemi-MPO to a much lesser extent than dimeric
 MPO-stimulated rise in cytosolic calcium and lysozyme exo-
 cytosis in neutrophils, and the capacity of monomeric MPO
 to delay apoptosis of neutrophils and increase their lifespan
 was weaker than that of dimeric MPO [20].

Previous studies with RBCs demonstrated that MPO-
 HOCl, in contrast to native dimeric MPO, lost its ability

516 to bind to plasma membrane of RBC and regulate their
517 structural and functional properties [13]. Apparently, this
518 effect was due to a decrease in the net positive charge
519 of the MPO molecule, resulted from halogenation of its
520 amino groups by HOCl, that led to a decrease in the elec-
521 trostatic interaction with negatively charged RBC plasma
522 membrane proteins. In present study, we have shown for
523 the first time that in contrast to MPO-HOCl [13], hemi-
524 MPO, obtained from native MPO by disulfide cleavage,
525 retained the ability of the enzyme to bind to RBC surface
526 (Fig. 1). Since dimeric MPO dissociation into two hemi-
527 MPO molecules due to disulfide bond reduction preserves
528 the charge of the hemi-MPO molecules, then, apparently,
529 the electrostatic interaction of hemi-MPO with RBC pro-
530 teins is conserved.

531 Binding of hemi-MPO, as well as binding of dimeric
532 MPO with RBC's membrane proteins, reduced cell resist-
533 ance to osmotic and acidic hemolysis as well as cell elastic-
534 ity (Fig. 2), led to significant changes in cell volume, mor-
535 phology (Table 1, Figs. 3, 4), the conductance of plasma
536 membrane ion channels (Fig. 5) and cytosolic Ca^{2+} concen-
537 tration of RBCs (Fig. 6). It has been shown for the first time
538 that both dimeric and hemi-MPO contribute to the forma-
539 tion of PS-positive RBCs (Fig. 7). These results are of great
540 importance, as the exposure of PS on the outer membrane
541 leaflet of RBCs serves as a signal for eryptosis, a mechanism
542 for the RBC clearance from blood circulation and also lead
543 to adhesion of RBCs to endothelium in some diseases such
544 as sickle cell anemia, malaria, and diabetes [41].

545 However, the effects of hemi-MPO on the structural and
546 functional properties of RBCs were lower compared with
547 those of dimeric MPO. The possible reason is the presence
548 of two receptor-binding sites on native dimeric MPO mol-
549 ecule in contrast to one binding site for hemi-MPO. Dimeric
550 MPO, being a bivalent ligand, when binds to its correspond-
551 ing receptors, can lead to their clustering that may have a
552 significant effect on intracellular signaling [42, 43]. On the
553 other hand, it was shown that MPO-binding proteins on
554 RBC membrane: band 3 protein and glycophorin A, form
555 a complex [44, 45]. Furthermore, as bivalent ligands may
556 possess higher binding affinity to clustered receptors com-
557 pared to monovalent ligands [42, 43], dimeric MPO effect on
558 the structural and functional RBC properties may be more
559 pronounced compared to hemi-MPO.

560 Thus, the ability of MPO protein to influence RBC's bio-
561 physical properties depends on its conformation (dimeric or
562 monomeric isoform). It is intriguing to speculate that hemi-
563 MPO appearance in blood during inflammation, as it was
564 shown earlier [20], can serve as a regulatory mechanism
565 addressed to reduce abnormalities on RBC response.

566 **Acknowledgements** This work was partly supported by Russian Foun-
567 dation for Basic Research (Grant 18-515-00004, Grant 17-54-04009)

and Belarusian Republican Foundation for Fundamental Research
568 (Grant B18R-058). 569

570 Compliance with ethical standards

Conflict of interest The authors declare no competing financial and
571 nonfinancial interests. 572

Ethical approval This work was approved by the protocol of the Local
573 Ethics Committee at Federal State Budgetary Scientific Institution
574 "Institute of Experimental Medicine". 575

576 References

- 577 Furtmüller PG, Burner U, Obinger C (1998) Reaction of mye-
578 loperoxidase compound I with chloride, bromide, iodide, and
579 thiocyanate. *Biochemistry* 37(51):17923–17930. <https://doi.org/10.1021/bi9818772>
- 580 Davies MJ, Hawkins CL, Pattison DI, Rees MD (2008) Mam-
581 malian heme peroxidases: from molecular mechanisms to health
582 implications. *Antioxid Redox Signal* 10(7):1199–1234. <https://doi.org/10.1089/ars.2007.1927>
- 583 Morgan PE, Pattison DI, Talib J, Summers FA, Harmer JA, Cel-
584 ermajer DS, Hawkins CL, Davies MJ (2011) High plasma thio-
585 cyanate levels in smokers are a key determinant of thiol oxidation
586 induced by myeloperoxidase. *Free Radic Biol Med* 51(9):1815–
587 1822. <https://doi.org/10.1016/j.freeradbiomed.2011.08.008>
- 588 Chandler JD, Day BJ (2015) Biochemical mechanisms and thera-
589 peutic potential of pseudohalide thiocyanate in human health.
590 *Free Radic Res* 49(6):695–710. <https://doi.org/10.3109/10715762.2014.1003372>
- 591 Pattison DI, Davies MJ (2006) Reactions of myeloperoxidase-
592 derived oxidants with biological substrates: gaining chemical
593 insight into human inflammatory diseases. *Curr Med Chem*
594 13(27):3271–3290. <https://doi.org/10.2174/092986706778773095>
- 595 Panasenکو OM, Gorudko IV, Sokolov AV (2013) Hypochlorous
596 acid as a precursor of free radicals in living systems. *Biochemis-
597 try (Moscow)* 78(13):1466–1489. <https://doi.org/10.1134/S0006297913130075>
- 598 Panasenکو OM, Sergienko VI (2010) Halogenizing stress and
599 its biomarkers [Article in Russian]. *Vestn Ross Akad Med Nauk*
600 1:27–39
- 601 Yap YW, Whiteman M, Cheung NS (2007) Chlorinative stress:
602 an under appreciated mediator of neurodegeneration? *Cell Signal*
603 19(2):219–228. <https://doi.org/10.1016/j.cellsig.2006.06.013>
- 604 Gorudko IV, Sokolov AV, Shamova EV, Grudinina NA, Drozd ES,
605 Shishlo LM, Grigorieva DV, Bushuk SB, Bushuk BA, Chizhik
606 SA, Cherenkevich SN, Vasilyev VB, Panasenکو OM (2013)
607 Myeloperoxidase modulates human platelet aggregation via actin
608 cytoskeleton reorganization and store-operated calcium entry. *Biol*
609 *Open* 2(9):916–923. <https://doi.org/10.1242/bio.20135314>
- 610 Kolarova H, Klinke A, Kremserova S, Adam M, Pekarova M,
611 Baldus S, Eiserich JP, Kubala L (2013) Myeloperoxidase induces
612 the priming of platelets. *Free Radic Biol Med* 61:357–369. <https://doi.org/10.1016/j.freeradbiomed.2013.04.014>
- 613 Klinke A, Nussbaum C, Kubala L, Friedrichs K, Rudolph TK,
614 Rudolph V, Paust HJ, Schröder C, Bente D, Lau D, Szocs K,
615 Furtmüller PG, Heeringa P, Sydow K, Duchstein HJ, Ehmke
616 H, Schumacher U, Meinertz T, Sperandio M, Baldus S (2011)
617 Myeloperoxidase attracts neutrophils by physical forces. *Blood*
618 117(4):1350–1358. <https://doi.org/10.1182/blood-2010-05-284513>

- 625 12. Lau D, Mollnau H, Eiserich JP, Freeman BA, Daiber A, Gehling
626 UM, Brümmer J, Rudolph V, Münzel T, Heitzer T, Meinertz T,
627 Baldus S (2005) Myeloperoxidase mediates neutrophil activa-
628 tion by association with CD11b/CD18 integrins. *Proc Natl Acad*
629 *Sci USA* 102(2):431–436. [https://doi.org/10.1073/pnas.04051](https://doi.org/10.1073/pnas.0405193102)
630 [93102](https://doi.org/10.1073/pnas.0405193102)
- 631 13. Gorudko IV, Sokolov AV, Shamova EV, Grigorieva DV, Mironova
632 EV, Kudryavtsev IV, Gusev SA, Gusev AA, Chekanov AV, Vasi-
633 lyev VB, Cherenkevich SN, Panasenکو OM, Timoshenko AV
634 (2016) Binding of human myeloperoxidase to red blood cells:
635 molecular targets and biophysical consequences at the plasma
636 membrane level. *Arch Biochem Biophys* 591:87–97. [https://doi.](https://doi.org/10.1016/j.abb.2015.12.007)
637 [org/10.1016/j.abb.2015.12.007](https://doi.org/10.1016/j.abb.2015.12.007)
- 638 14. Benson TW, Weintraub NL, Kim HW, Seigler N, Kumar S, Pye J,
639 Horimatsu T, Pellenberg R, Stepp DW, Lucas R, Bogdanov VY,
640 Litwin SE, Brittain JE, Harris RA (2018) A single high-fat meal
641 provokes pathological erythrocyte remodeling and increases mye-
642 loperoxidase levels: implications for acute coronary syndrome.
643 *Lab Invest* 98(10):1300–1310. [https://doi.org/10.1038/s4137](https://doi.org/10.1038/s41374-018-0038-3)
644 [4-018-0038-3](https://doi.org/10.1038/s41374-018-0038-3)
- 645 15. Blair-Johnson M, Fiedler T, Fenna R (2001) Human myelopero-
646 oxidase: structure of a cyanide complex and its interaction with
647 bromide and thiocyanate substrates at 1.9 Å resolution. *Biochem-*
648 *istry* 40(46):13990–13997. <https://doi.org/10.1021/bi0111808>
- 649 16. Yamada M, Mori M, Sugimura T (1981) Myeloperoxidase
650 in cultured human promyelocytic leukemia cell line HL-60.
651 *Biochem Biophys Res Commun* 98(1):219–226. [https://doi.](https://doi.org/10.1016/0006-291X(81)91891-X)
652 [org/10.1016/0006-291X\(81\)91891-X](https://doi.org/10.1016/0006-291X(81)91891-X)
- 653 17. Yamada M, Mori M, Sugimura T (1983) Myeloperoxidase of
654 human myeloid leukemia cells HL-60 grown in culture and in
655 nude mice. *J Biochem* 93(6):1661–1668
- 656 18. Andrews PC, Krinsky NI (1981) The reductive cleavage of mye-
657 loperoxidase in half, producing enzymically active hemi-myelop-
658 eroxidase. *J Biol Chem* 256(9):4211–4218
- 659 19. Gorudko IV, Mikhailchik EV, Sokolov AV, Grigorieva DV, Koste-
660 vich VA, Vasilyev VB, Cherenkevich SN, Panasenکو OM (2017)
661 The production of reactive oxygen and halogen species by neu-
662 trophils in response to monomeric forms of myeloperoxidase.
663 *Biophysics* 62(6):919–925. [https://doi.org/10.1134/S000635091](https://doi.org/10.1134/S0006350917060069)
664 [7060069](https://doi.org/10.1134/S0006350917060069)
- 665 20. Gorudko IV, Grigorieva DV, Sokolov AV, Shamova EV, Koste-
666 vich VA, Kudryavtsev IV, Syromiatnikova ED, Vasilyev VB,
667 Cherenkevich SN, Panasenکو OM (2018) Neutrophil activation
668 in response to monomeric myeloperoxidase. *Biochem Cell Biol*
669 96(5):592–601. <https://doi.org/10.1139/bcb-2017-0290>
- 670 21. Zuurbier KW, van den Berg JD, Van Gelder BF, Muijsers AO
671 (1992) Human hemi-myeloperoxidase. Initial chlorinating activ-
672 ity at neutral pH, compound II and III formation, and stability
673 towards hypochlorous acid and high temperature. *Eur J Biochem*
674 205(2):737–742. [https://doi.org/10.1111/j.1432-1033.1992.tb168](https://doi.org/10.1111/j.1432-1033.1992.tb16837.x)
675 [37.x](https://doi.org/10.1111/j.1432-1033.1992.tb16837.x)
- 676 22. Gorudko IV, Cherkalina OS, Sokolov AV, Pulina MO, Zakharova
677 ET, Vasilyev VB, Cherenkevich SN, Panasenکو OM (2009) New
678 approaches to the measurement of the concentration and peroxi-
679 dase activity of myeloperoxidase in human blood plasma. *Bioorg*
680 *Khim* 35(5):629–639. [https://doi.org/10.1134/S10681620090500](https://doi.org/10.1134/S1068162009050057)
681 [57 \(Russian\)](https://doi.org/10.1134/S1068162009050057)
- 682 23. Hope HR, Remsen EE, Lewis C Jr, Heuvelman DM, Walker MC,
683 Jennings M, Connolly DT (2000) Large-scale purification of mye-
684 loperoxidase from HL60 promyelocytic cells: characterization and
685 comparison to human neutrophil myeloperoxidase. *Protein Expr*
686 *Purif* 18(3):269–276. <https://doi.org/10.1006/prep.1999.1197>
- 687 24. Sokolov AV, Kostevich VA, Zakharova ET, Samygina VR,
688 Panasenکو OM, Vasilyev VB (2015) Interaction of ceruloplas-
689 min with eosinophil peroxidase as compared to its interplay with
690 myeloperoxidase: reciprocal effect on enzymatic properties.
691 *Free Radic Re* 49(6):800–811. [https://doi.org/10.3109/10715](https://doi.org/10.3109/10715762.2015.1005615)
692 [762.2015.1005615](https://doi.org/10.3109/10715762.2015.1005615)
- 693 25. Vakhrusheva TV, Sokolov AV, Kostevich VA, Vasilyev VB,
694 Panasenکو OM (2018) Enzymatic and bactericidal activity of
695 monomeric and dimeric forms of myeloperoxidase. *Biochem*
696 *Moscow Suppl Ser B* 12(3):258–265. [https://doi.org/10.1134/](https://doi.org/10.1134/S1990750818030083)
697 [S1990750818030083](https://doi.org/10.1134/S1990750818030083)
- 698 26. Fling SP, Gregerson DS (1986) Peptide and protein molecular
699 weight determination by electrophoresis using a high-molarity tris
700 buffer system without urea. *Anal Biochem* 155(1):83–88. [https://](https://doi.org/10.1016/0003-2697(86)90228-9)
701 [doi.org/10.1016/0003-2697\(86\)90228-9](https://doi.org/10.1016/0003-2697(86)90228-9)
- 702 27. Anderson NL, Nance SL, Pearson TW, Anderson NG (1982)
703 Two-dimensional electrophoretic patterns of human plasma
704 membrane proteins immobilized on nitrocellulose. *Electropho-*
705 *resis* 3:135–142
- 706 28. Sokolov AV, Pulina MO, Ageeva KV, Tcherkalina OS, Zakharova
707 ET, Vasilyev VB (2009) Identification of complexes formed by
708 ceruloplasmin with matrix metalloproteinases 2 and 12. *Biochem-*
709 *istry (Mosc)* 74(12):1388–1392. [https://doi.org/10.1134/S0006](https://doi.org/10.1134/S0006297909120141)
710 [297909120141](https://doi.org/10.1134/S0006297909120141)
- 711 29. Drozd ES, Chizhik SA (2008) Combined atomic force microscopy
712 and optical microscopy measurements as a method of erythrocyte
713 investigation. *Proc SPIE*. <https://doi.org/10.1117/12.836481>
- 714 30. Mathur AB, Collinsworth AM, Reichert WM, Kraus WE, Trus-
715 key GA (2001) Endothelial, cardiac muscle and skeletal muscle
716 exhibit different viscous and elastic properties as determined by
717 atomic force microscopy. *J Biomech* 34(12):1545–1553. [https://](https://doi.org/10.1016/S0021-9290(01)00149-X)
718 [doi.org/10.1016/S0021-9290\(01\)00149-X](https://doi.org/10.1016/S0021-9290(01)00149-X)
- 719 31. Adam M, Gajdova S, Kolarova H, Kubala L, Lau D, Geisler
720 A, Ravekes T, Rudolph V, Tsao PS, Blankenberg S, Baldus S,
721 Klinke A (2014) Red blood cells serve as intravascular carriers
722 of myeloperoxidase. *J Mol Cell Cardiol* 74:353–363. [https://doi.](https://doi.org/10.1016/j.yjmcc.2014.06.009)
723 [org/10.1016/j.yjmcc.2014.06.009](https://doi.org/10.1016/j.yjmcc.2014.06.009)
- 724 32. Gorudko IV, Cherkalina OS, Sokolov AV, Pulina MO, Zakharova
725 ET, Vasilyev VB, Cherenkevich SN, Panasenکو OM (2009) New
726 approaches to the measurement of the concentration and peroxi-
727 dase activity of myeloperoxidase in human blood plasma. *Bioorg-*
728 *an Khim* 35:629–639
- 729 33. Zavodnik LB, Zavodnik IB, Lapshyna EA, Buko VU, Bryszewska
730 MJ (2002) Hypochlorous acid-induced membrane pore formation
731 in red blood cells. *Bioelectrochemistry* 58(2):157–161. [https://doi.](https://doi.org/10.1016/S1567-5394(02)00151-2)
732 [org/10.1016/S1567-5394\(02\)00151-2](https://doi.org/10.1016/S1567-5394(02)00151-2)
- 733 34. Zavodnik LB, Zavodnik IB, Lapshyna EA, Shkodich AP, Brysz-
734 ewska M, Buko VU (2000) Hypochlorous acid-induced lysis
735 of human erythrocytes. Inhibition of cellular damage by the
736 isoflavonoid genistein-8-C-glucoside. *Biochemistry (Mosc)*
737 65(8):946–951
- 738 35. Bevers EM, Williamson PL (2010) Phospholipid scramblase: an
739 update. *FEBS Lett* 584(13):2724–2730. [https://doi.org/10.1016/j.](https://doi.org/10.1016/j.febslet.2010.03.020)
740 [febslet.2010.03.020](https://doi.org/10.1016/j.febslet.2010.03.020)
- 741 36. Wesseling MC, Wagner-Britz L, Huppert H, Hanf B, Hertz L,
742 Nguyen DB, Bernhardt I (2016) Phosphatidylserine exposure in
743 human red blood cells depending on cell age. *Cell Physiol Bio-*
744 *chem* 38(4):1376–1390. <https://doi.org/10.1159/000443081>
- 745 37. Jacobi J, Lang E, Bissinger R, Frauenfeld L, Modicano P, Faggio
746 C, Abed M, Lang F (2014) Stimulation of erythrocyte cell mem-
747 brane scrambling by mitotane. *Cell Physiol Biochem* 33(5):1516–
748 1526. <https://doi.org/10.1159/000358715>
- 749 38. Nguyen DB, Wagner-Britz L, Maia S, Steffen P, Wagner C, Kaes-
750 tner L, Bernhardt I (2011) Regulation of phosphatidylserine expo-
751 sure in red blood cells. *Cell Physiol Biochem* 28(5):847–856. [https://doi.](https://doi.org/10.1159/000335798)
752 [org/10.1159/000335798](https://doi.org/10.1159/000335798)
- 753 39. Kebir D, József L, Pan W, Filep JG (2008) Myeloperoxidase
754 delays neutrophil apoptosis through CD11b/CD18 integrins and
755 prolongs inflammation. *Circ Res* 103(4):352–359. [https://doi.](https://doi.org/10.1161/01.RES.0000326772.76822.7a)
756 [org/10.1161/01.RES.0000326772.76822.7a](https://doi.org/10.1161/01.RES.0000326772.76822.7a)

- 757 40. Johansson MW, Patarroyo M, Oberg F, Siegbahn A, Nils-
758 son K (1997) Myeloperoxidase mediates cell adhesion via the
759 alpha M beta 2 integrin (Mac-1, CD11b/CD18). *J Cell Sci*
760 110(Pt9):1133–1139
- 761 41. Closse C, Dachary-Prigent J, Boisseau MR (1999) Phosphati-
762 dylserine-related adhesion of human erythrocytes to vascular
763 endothelium. *Br J Haematol* 107:300–302. <https://doi.org/10.1046/j.1365-2141.199.01718.x>
- 764 42. Grochmal A, Ferrero E, Milanesi L, Tomas S (2013) Modula-
765 tion of in-membrane receptor clustering upon binding of multi-
766 valent ligands. *J Am Chem Soc* 135(27):10172–10177. <https://doi.org/10.1021/ja404428u>
- 767 43. Jung H, Robison AD, Cremer PS (2009) Multivalent ligand-recep-
768 tor binding on supported lipid bilayers. *J Struct Biol* 168(1):90–
769 94. <https://doi.org/10.1016/j.jsb.2009.05.010>
- 770 44. Nigg EA, Bron C, Girardet M, Cherry RJ (1980) Band 3-gly-
771 cophorin A association in erythrocyte membrane demonstrated
772 by combining protein diffusion measurements with antibody-
773 induced cross-linking. *Biochemistry* 19(9):1887–1893. <https://doi.org/10.1021/bi00550a024>
- 774 45. Auffray I, Marfatia S, de Jong K, Lee G, Huang CH, Paszty
775 C, Tanner MJ, Mohandas N, Chasis JA (2001) Glycophorin A
776 dimerization and band 3 interaction during erythroid membrane
777 biogenesis: in vivo studies in human glycophorin A transgenic
778 mice. *Blood* 97(9):2872–2878. <https://doi.org/10.1182/blood.V97.9.2872>
- 779
780
781
782
- Publisher's Note** Springer Nature remains neutral with regard to
783 jurisdictional claims in published maps and institutional affiliations.
784
- 785

UNCORRECTED PROOF

Journal:	11010
Article:	3654

Author Query Form

Please ensure you fill out your response to the queries raised below and return this form along with your corrections

Dear Author

During the process of typesetting your article, the following queries have arisen. Please check your typeset proof carefully against the queries listed below and mark the necessary changes either directly on the proof/online grid or in the 'Author's response' area provided below

Query	Details Required	Author's Response
AQ1	Journal instruction requires a city and country for affiliations; however, these are missing in affiliations [5, 6]. Please verify if the provided city and country are correct and amend if necessary.	
AQ2	Figures: figures (3,4a) are poor in quality as its labels are not readable. Please supply a new version of the said figure with legible labels preferably in .eps, .tiff or .jpeg format with 600 dpi resolution.	

Author Proof